

### Axially enhanced far field and radiation flux in a magnetoplasma

H. M. Lai, C. S. Ng, and S. S. Tong

Department of Physics, The Chinese University of Hong Kong, Hong Kong

(Received 26 January 1989)

Conditions for the existence of an inversely (distance)<sup>1/2</sup>-dependent far field along the direction of the external magnetic field in a cold magnetoplasma are studied and applied to classify the plasma parameter domains in the Clemmow-Mullaly-Allis diagram. Such an *axially enhanced* far-field flux from a dipole source is then evaluated explicitly and found to be confined within a finite cross-sectional area in most cases. Origin of the axial enhancement is explained and its relevance to energy conservation is discussed; in particular, the divergent radiation flux lines are described by  $z/r_1^2 = \text{const}$ , where  $z$  and  $r_1$  are, respectively, the axial and the transverse coordinates. Attention is also drawn to the existence of an enhanced electric far field oscillating *parallel* to the magnetic field and at frequencies *below* the plasma frequency.

#### I. INTRODUCTION

It is well known that the far field (i.e., the field in the far zone) caused by a radiating source in a homogeneous, isotropic, and loss-free medium is inversely proportional to the distance as required by the law of energy conservation. However, for a source in an *anisotropic* medium, this simple inverse relation may fail to hold along certain angular directions. Lighthill,<sup>1</sup> in a paper mainly addressed to the calculation of the far field due to a monochromatic source, appears to be the first one to have shown the existence of this peculiarity. His method, followed and developed by Giles,<sup>2</sup> consists of the following steps. First, only the excited waves satisfying the dispersion relation are shown to contribute to the far field which can then be expressed as an integral over the wave-vector surface (WS); a WS is the surface in the wave-vector space satisfying the dispersion relation for a given frequency. Secondly, the integral is evaluated by applying the standard method of stationary phase to the WS and the result for the far field, depending inversely on the square root of the Gaussian curvature  $K$  of the WS at the point of stationary phase, can be interpreted as the interference maximum of the excited waves whose group velocity is directed towards the observer. Finally, and more interestingly, in the special case where  $K=0$ , the far field is shown to be inversely proportional to either  $r^{5/6}$  or  $r^{1/2}$ , where  $r$  is the distance between the source and the observer. It should be pointed out that such a peculiar dependence, valid only in the direction of the group velocity at the point of stationary phase with zero Gaussian curvature, by no means holds within a finite solid angle and thus has no contradiction with the law of energy conservation.

For a cold plasma in a uniform external magnetic field  $\mathbf{B} = B_0 \hat{\mathbf{z}}$ , the WS is a surface of rotation of the  $k_z$ -vs- $k_x$  dispersion curve (for a given frequency) about the  $z$  axis, whose direction will also be referred to as the axial direction;  $k_x$  and  $k_z$  are the two components of the wave vector in the  $x$ - $z$  plane. Three cases of zero Gaussian curvature have been shown:<sup>1,2</sup> (i) the resonance cone case<sup>3</sup>

where the wave number goes to infinity at a finite polar angle and thermal effects have to be included;<sup>4</sup> (ii) the case of an inflection point on the dispersion curve; and (iii) the case of an extremum of  $k_z$  at a *nonzero*  $k_x$  [Fig. 1(a)] so that there is a *ring* of extrema on the WS. However, there is the fourth case where the ring coalesces to the pole and the derivatives of  $k_z$  with respect to  $k_x$  are zero up to the third order, rendering a zero  $K$  at the two poles of the WS [Fig. 1(b)]. As we shall see, the last two cases need separate consideration and they are of particular interest because they both lead to an inverse  $r^{1/2}$  dependence of the far field along the axial direction of the WS and hence possibly a much enhanced radiation.

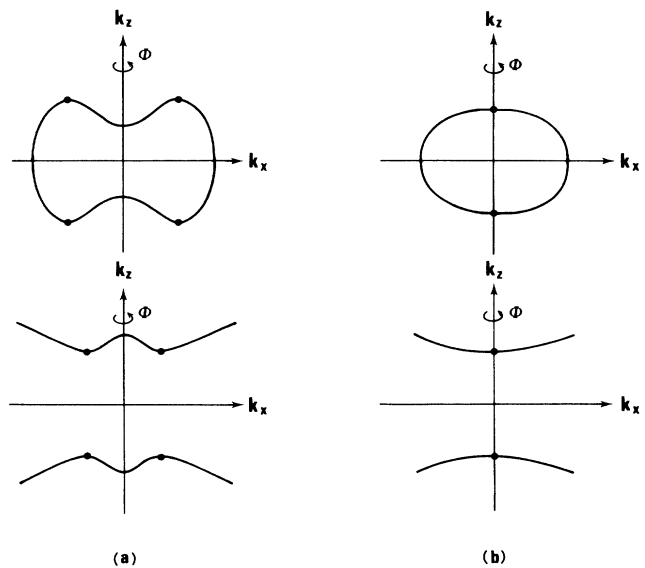


FIG. 1. Dispersion curves, the WS of each is a surface of rotation. (a) Extremum  $k_z$  at a nonzero  $k_x$ , forming a ring on the WS; (b) extremum ring coalescing to the point at  $k_x = 0$ , giving rise to a quasiflat surface near each of the poles on the WS.

The present paper is addressed to the study of this *axially enhanced far field* (AEFF) and related problems. In Sec. II we shall classify analytically the plasma parameter domains in the well-known Clemmow-Mullaly-Allis (CMA) diagram where such an AEFF phenomenon could occur, taking into account the ion motions. The result obtained can be seen as a supplement and an extension to the earlier work by Giles,<sup>2</sup> who had made the classification in a numerical way and had restricted to the high-frequency regime. In Sec. III we start by a brief review of Lighthill's method in the context of a source in a cold magnetoplasma, while introducing notations and supplying explanations to be used later on. We next consider the AEFF situation and calculate explicitly the far field on the  $z$  axis caused by an electric dipole source at the origin; for a dipole oriented along the  $z$  axis, we show the existence of an enhanced electric far field on the axis oscillating *longitudinally* (i.e., parallel to the external magnetic field) at frequencies *less* than the plasma frequency. Assuming the case of a ring of extrema on the WS (i.e., the third case), the enhanced far field *around* the axis is calculated and it is found mainly confined within a constant cross section of the size of the transverse wavelength. Explanations for the inverse  $r^{1/2}$  dependence and the parallel oscillation at subplasma frequencies are given. In Sec. IV we calculate the radiation energy flux and discuss the problem of energy conservation in view of the inverse  $r$  dependence. Conclusions and further remarks are given in Sec. V.

### II. CMA DOMAINS WITH AXIALLY ENHANCED FAR FIELD (AEFF)

For a two-component cold magnetoplasma, the  $k_z$ - $k_x$  dispersion curve for a given frequency  $\omega$  is determined essentially by

$$n_z^2 = S - (1 + S/P)n_x^2/2 \pm [h(n_x)]^{1/2}, \quad (1a)$$

with

$$h(n_x) \equiv (1 - S/P)^2 n_x^4/4 + D^2(1 - n_x^2/P), \quad (1b)$$

where the "refractive-index vector" or the dimensionless wave vector

$$\mathbf{n} \equiv c\mathbf{k}/\omega \quad (1c)$$

has been defined with  $c$  being the speed of light in vacuum, and<sup>5</sup>

$$S = (R + L)/2, \quad D = (R - L)/2, \quad P = 1 - X, \quad (2a)$$

$$R = 1 - X / [(1 - Y)(1 + mY/M)], \quad (2b)$$

$$L = 1 - X / [(1 + Y)(1 - mY/M)], \quad (2c)$$

$$X = \omega_p^2/\omega^2, \quad Y = \Omega_e/\omega, \quad (2c)$$

with  $m$  ( $M$ ),  $\Omega_e$ , and  $\omega_p = (\omega_{pe}^2 + \omega_{pi}^2)^{1/2}$  being, respectively, the electron (ion) mass, the electron gyrofrequency and the plasma frequency; a singly ionized plasma has been assumed. Clearly, the dispersion curve is meaningful only in the domain of  $k_x$  where the right-hand side of

Eq. (1a) is positive. Because a WS is a surface of rotation of the  $k_z$ - $k_x$  curve about the  $z$  axis and has reflection symmetry with respect to the  $k_z=0$  plane, it may be graphically represented by the  $k_z$ - $k_x$  (or  $n_z$ - $n_x$ ) dispersion curve given by Eq. (1a) in the first quadrant. Furthermore, the appearance of two solutions means that the WS could be two-sheeted.

To find the parameter domain where there is an extremum of  $k_z$  at nonzero  $k_x$  in the first quadrant, we reproduce the CMA diagram in Fig. 2 where the mass ratio  $M/m$  has been set equal to 10 for the convenience of displaying the graphs. The solid curves (given by  $L=0$ ,  $R=0$ ,  $P=0$ ,  $Y=1$  and 10) are the usual ones dividing the diagram into various "ponds," while the small  $k_z$ - $k_x$  graphs (in the first quadrant) in each pond, representing the wave-vector surfaces in a topological way, replace the usual phase-velocity surfaces; the two kinds of surfaces are related by an inversion with respect to a sphere around the origin. The numbering of the ponds follows that of Stix.<sup>5</sup> We note the following known properties of the WS's: (i) topologically, a WS must be either an ellipsoid, a two-sheeted hyperboloid, or a one-sheeted hyperboloid; (ii) there is no two-sheeted hyperboloidal WS for  $X < 1$ ; (iii) in the  $k_x$ - $k_z$  plane, there are at most two posi-

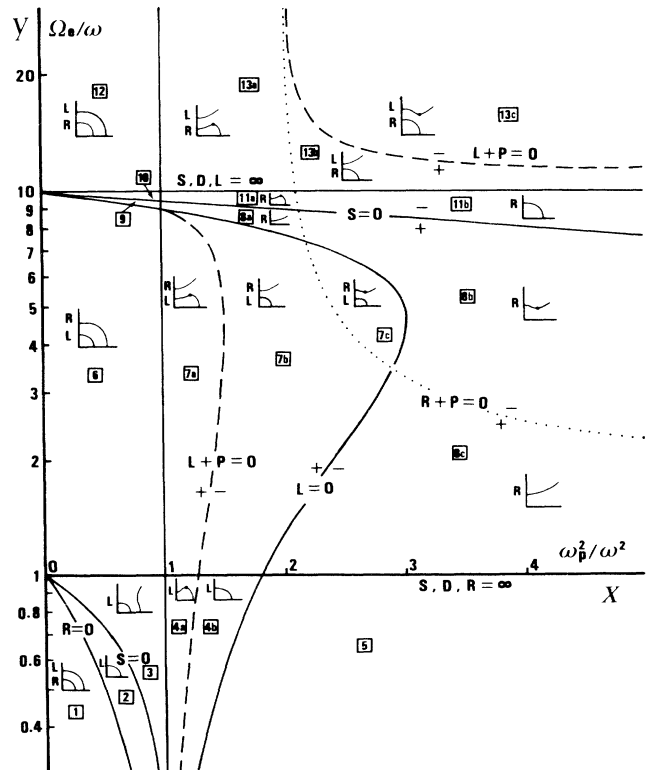


FIG. 2. The usual 13 CMA domains (defined by the solid lines) and the AEFF subdomains 4a, 7a, 7c, 8b, 11a, 13a, and 13c (defined by the dashed lines). Mass ratio is set to 10. Graphs in the first quadrant indicate the shape of the WS in each subdomain.

tive values of  $k_x$  for a given  $k_z$ . Property (iii) immediately rules out the one-sheeted hyperboloidal WS to have an extremum of  $k_z$  versus  $k_x$ . It is also not difficult to see that, for an ellipsoidal WS,  $k_z$  must be minimum at  $k_x=0$  in order to have an extremum (which is a maximum) at a nonzero  $k_x$  without contradicting property (iii), whereas for a two-sheeted hyperboloidal WS,  $k_z$  must be maximum at  $k_x=0$  in order to have an extremum (which is a minimum) at a nonzero  $k_x$ . Now we have, from Eq. (1a), the following relation:

$$dn_z/dn_x \simeq -n_x(1+n_0^2/P)/2n_z \quad (3)$$

in the neighborhood of the origin, where  $n_0^2=R$  or  $L$  is the square of the refractive index for waves propagating along the magnetic field. Therefore, for an ellipsoidal WS,  $P < 0$  must be satisfied. Together with property (ii) and the implication from property (iii), we may conclude that AEFf exists only in the region of  $P < 0$  or  $X > 1$ . In other words, AEFf is possible only if the wave frequency is *below* the plasma frequency. Moreover, for an  $R$ -labeled (or an  $L$ -labeled) ellipsoidal WS, the further condition from Eq. (3) is  $R+P > 0$  (or  $L+P > 0$ ) whereas, for an  $R$ -labeled (or an  $L$ -labeled) two-sheeted hyperboloidal WS, it is  $R+P < 0$  (or  $L+P < 0$ ); an  $R$ - or  $L$ -labeled WS is that which describes the right-handed or left-handed circularly polarized wave at  $k_x=0$ . In Fig. 2 the two dashed lines give  $L+P=0$  and the dotted line gives  $R+P=0$ ; the positive and negative side of each of these curves is also indicated for convenience. These lines divide the  $X > 1$  region into domains of far-field enhancement. For example, the CMA domain 7 (bounded by  $L=0$ ,  $P=0$ , and  $Y=1$ ) is divided into subdomains 7a, 7b, and 7c; since both an  $L$ -labeled ellipsoid and an  $R$ -labeled two-sheeted hyperboloid exist in the original domain, subdomain 7a (defined by  $L+P > 0$ ) gives rise to an “ $L$ -type” AEFf (associated with the  $L$ -labeled surface), whereas subdomain 7c (defined by  $R+P < 0$ ) gives rise to an “ $R$ -type” AEFf (associated with the  $R$ -labeled surface). Incidentally, we should like to point out that subdomain 7c exists only if  $M/m > 8.1$ . Similar analysis shows that subdomains 4a and 13c give rise to  $L$ -type AEFf’s while 8b, 11a, and 13a give rise to  $R$ -type AEFf’s. In total there are seven such subdomains. It is of interest to point out that, except for subdomain 13b, which is a relatively small domain (especially so for large  $M/m$ ), far-field enhancement along the external magnetic field direction always exists in the low-frequency region where  $Y > M/m$  (i.e.,  $\omega < \Omega_i$ , the ion gyrofrequency) and  $X > 1$  (i.e.,  $\omega < \omega_p$ ), and the ion motions have to be fully taken into account.

We now turn to the parameter points on the boundary line determined by  $R+P=0$ . At any such point, the second derivative  $d^2k_z/dk_x^2$  is zero at the origin for the  $R$ -labeled surface [see Eq. (3)]. Since WS is a surface of rotation, we conclude that the derivatives of  $k_z$  with respect to  $k_x$  at the origin are zero up to the third order and the pole surface is almost flat. A similar conclusion can be achieved for a parameter point on the boundary lines of  $L+P=0$ . In particular, we have, from Eq. (1a), the following expansion:

$$n_z = |P|^{1/2} + \alpha n_x^4/4 \quad (4a)$$

around  $n_x=0$  or  $k_x=0$ , where

$$\alpha = \pm S/(D|P|^{3/2}) \quad (4b)$$

is the coefficient with the plus sign corresponding to the case of  $R=-P$  and the minus sign for the case of  $L=-P$ . It is not difficult to see that  $\alpha$  is positive (or negative) for a two-sheeted hyperboloidal (or an ellipsoidal) WS.

Finally, the exact position of the extremum in each subdomain of AEFf can be calculated. By solving  $dn_z/dn_x=0$ , only one real root of positive  $n_x$  is found and it is equal to

$$v_1 = \frac{\{2PD^2 + |D(1+P/S)|[SP(P-R)(L-P)]^{1/2}\}^{1/2}}{|S-P|} \quad (5a)$$

and the corresponding  $n_z$  is obtained to be

$$v_2 = |\{PD \pm [PS(P-R)(L-P)]^{1/2}\}/(S-P)|P|^{1/2}|, \quad (5b)$$

where  $P < 0$  has been assumed. Since there is only one extremum value, one still has to make a choice between the two values in Eq. (5b). To this aim, we note that in Fig. 2, as the boundary line  $R=-P$  (or  $L=-P$ ) is approached by any parameter point  $(X, Y)$  in a nearby subdomain of AEFf,  $v_1$  will tend to zero and the extremum value must be  $\sqrt{R}$  (or  $\sqrt{L}$ ). Such a criterion leads to the choice of the plus sign in Eq. (5b) for subdomains 7a, 11a, and 13c and the choice of the minus sign for 4a, 7c, 8b, and 13a, in order to have  $v_2$  as the proper extremum value. (Note that  $D$  is positive in between  $Y=1$  and  $Y=M/m$ , and is negative otherwise.)

### III. FAR-FIELD EVALUATION

According to Lighthill,<sup>1</sup> Giles,<sup>2</sup> and Lai and Chan,<sup>6</sup> the far field  $\mathbf{E}(\mathbf{r})\exp(-i\omega t)$  at  $\mathbf{r}$  caused by a stationary source of current density  $\mathbf{J}(\mathbf{r})\exp(-i\omega t)$  located at the origin is given by the following integral over the wave-vector surface:

$$\mathbf{E}(\mathbf{r}) = (\omega^2/c^3\pi) \int_{\text{ws}} d^2n e^{i\mathbf{k}\cdot\mathbf{r}} \vec{\Gamma} \cdot \mathbf{J}(\mathbf{k}) / \frac{\partial \mathcal{D}}{\partial n_g}, \quad (6)$$

where  $\mathbf{J}(\mathbf{k})$  is the Fourier transform of  $\mathbf{J}(\mathbf{r})$ ,  $\mathcal{D}(\mathbf{k}, \omega)$  is the dispersion function equal to the determinant of the dispersion tensor

$$\Delta_{ij} = \epsilon_{ij}(\mathbf{k}, \omega) + n_i n_j - n^2 \delta_{ij} \quad (7)$$

( $\epsilon_{ij}$  being the dielectric tensor),  $\vec{\Gamma}$  is the adjoint of  $\vec{\Delta}$  (i.e., the matrix element  $\Gamma_{ij}$  is the cofactor of  $\Delta_{ji}$ ),  $\partial \mathcal{D} / \partial n_g \equiv (\omega/c)(\partial \mathcal{D} / \partial \mathbf{k})_g$  is the gradient of  $\mathcal{D}$  along the direction of the group velocity  $\mathbf{V}_g = \partial \omega(\mathbf{k}) / \partial \mathbf{k}$  [ $\omega(\mathbf{k})$  being the solution of  $\mathcal{D}(\mathbf{k}, \omega) = 0$ ], and the integration is over that part of the WS satisfying  $\mathbf{V}_g \cdot \mathbf{r} > 0$ . Since a wave-vector surface is essentially an “equal-frequency” surface [i.e., a surface given by  $\omega(\mathbf{k}) = \text{const}$ ], the group velocity, being the gradient of the frequency function, is

obviously normal to the surface. Physically, Eq. (6) shows that only the excited waves satisfying the dispersion relation contribute to the far field.

For a cold magnetoplasma the elements of the adjoint matrix are given by

$$\Gamma_{xx} = a_1 + a_2 \cos^2 \phi, \quad (8a)$$

$$\Gamma_{yy} = a_1 + a_2 \sin^2 \phi, \quad (8b)$$

$$\Gamma_{xy} = \Gamma_{yx}^* = a_2 \sin \phi \cos \phi + ia_3, \quad (8c)$$

$$\Gamma_{xz} = \Gamma_{zx}^* = -ia_4 \sin \phi + a_5 \cos \phi, \quad (8d)$$

$$\Gamma_{yz} = \Gamma_{zy}^* = ia_4 \cos \phi + a_5 \sin \phi, \quad (8e)$$

$$\Gamma_{zz} = a_6, \quad (8f)$$

where  $Q^*$  is the complex conjugate of  $Q$ ,  $\mathbf{n}$  is given in terms of the cylindrical coordinates  $n_\perp$ ,  $\phi$ , and  $n_z$ , and

$$a_1 = SP - Sn_\perp^2 - Pn_z^2, \quad (9a)$$

$$a_2 = n_\perp^2(n^2 - P), \quad (9b)$$

$$a_3 = D(P - n_\perp^2), \quad (9c)$$

$$a_4 = Dn_z n_\perp, \quad (9d)$$

$$a_5 = (n^2 - S)n_z n_\perp, \quad (9e)$$

$$a_6 = (S - n^2)(S - n_z^2) - D^2, \quad (9f)$$

are real and  $\phi$  independent. The dispersion function is equal to

$$\mathcal{D}(\mathbf{k}, \omega) = [n_z^2 - f_+(n_\perp, \omega)][n_z^2 - f_-(n_\perp, \omega)]P, \quad (10)$$

where  $f_\pm$  are the two functions on the right-hand side of Eq. (1a) with  $n_x$  replaced by  $n_\perp$ , and the WS may thus be represented parametrically in terms of  $n_\perp$  and  $\phi$  by

$$\mathbf{n} = n_\perp \hat{\rho} + n_z(n_\perp) \hat{z}, \quad (11)$$

where  $\hat{\rho} = \hat{x} \cos \phi + \hat{y} \sin \phi$  and  $n_z(n_\perp)$  is simply the square root of  $f_+$  or  $f_-$ . Bearing in mind that  $\mathbf{V}_g \cdot \mathbf{k} > 0$  for a spatially nondispersive medium,<sup>6</sup> it is not difficult to show, except for the one-sheeted hyperboloidal WS,

$$\hat{\mathbf{g}} = (\hat{z} - n_z' \hat{\rho}) / [1 + (n_z')^2]^{1/2} \quad (12)$$

is the unit vector normal to the WS and parallel to  $\mathbf{V}_g$ , and the parametric coordinate lines on the surface are the lines of curvature,<sup>6</sup> with the Gaussian curvature expressed as

$$K = |\lambda_\perp \lambda_\phi| \quad (13)$$

where

$$\lambda_\perp = \frac{(\partial^2 \mathbf{n} / \partial n_\perp^2)_g}{(\partial \mathbf{n} / \partial n_\perp)^2} = n_z'' / (1 + n_z'^2)^{3/2}, \quad (14a)$$

$$\lambda_\phi = \frac{(\partial^2 \mathbf{n} / \partial \phi^2)_g}{(\partial \mathbf{n} / \partial \phi)^2} = n_z' / [n_\perp (1 + n_z'^2)^{1/2}], \quad (14b)$$

are the two principal curvatures, with  $n_z'$  and  $n_z''$  being the derivatives with respect to  $n_\perp$ . Note that the two

principal curvatures become equal to each other as one approaches the pole on the WS and thus  $K$ , defined by Eqs. (13) and (14), again gives the correct Gaussian curvature at the pole even though the coordinates  $n_\perp$  and  $\phi$  are ill-defined there.

As shown by Lighthill,<sup>1</sup> the method of stationary phase implies that the contribution to the far field at  $\mathbf{r}$  in Eq. (6) comes mainly from the points on the WS where the surface normals are directed towards  $\mathbf{r}$ . If the Gaussian curvature  $K$  at every such point is nonzero, the far field has been shown to be equal to

$$\mathbf{E}(\mathbf{r}) = [\omega / (c^2 r)] \sum_{n_\sigma} \left[ \frac{2A}{K^{1/2}} \frac{\vec{\Gamma} \cdot \mathbf{J}}{\partial \mathcal{D} / \partial n_g} e^{ik \cdot \mathbf{r}} \right]_{n_\sigma}, \quad (15)$$

which is the sum of contributions from all such points  $n_\sigma$  where  $\hat{\mathbf{g}}$  is parallel to  $\mathbf{r}$ , the coefficient  $A$  being given by

$$A = \exp[(i\pi/4)(\lambda_\perp / |\lambda_\perp| + \lambda_\phi / |\lambda_\phi|)]. \quad (16)$$

We have seen, in Eq. (6), that the far field is a linear superposition of plane sinusoidal waves satisfying the dispersion relation, but here we obtain a result which is inversely proportional to the distance  $r$ . Although the  $1/r$  dependence is not unexpected, its origin is nonetheless worth pursuing and, as we shall see, its understanding helps to explain the existence of  $1/\sqrt{r}$ -dependent far field later on. In fact, the answer lies in the method of stationary phase in which the surface integral in Eq. (6) is reduced to a product of two line integrals each of the following form:

$$\int du \exp(i\lambda_u r u^2),$$

where  $u$  is essentially  $n_\perp$  or  $\phi$  and the integration domain is around the point of stationary phase. Because  $r$  is large, the dominant contribution comes from the central domain of width  $(\lambda_u r)^{-1/2}$ . This naturally leads to the following interpretation. The far field comes from those plane waves whose wave vectors end on a small element of the WS around the point of stationary phase, other waves simply superposing more or less in a destructive way and making a negligible contribution. The effective area of this element is the product of  $(\lambda_\perp r)^{-1/2}$  and  $(\lambda_\phi r)^{-1/2}$ , corresponding to the two effective widths. The larger the distance, the smaller the effective area and thus fewer sinusoidal waves contribute constructively to the far field. We see therefore that the inverse  $\sqrt{K}r$  dependence in Eq. (15) really stems from the size of the effective area or, more physically, it comes from the "number" of plane sinusoidal waves contributing to the far field in a constructive way.

From now on, we shall consider the case with a zero Gaussian curvature; in particular, we shall concentrate on the problem where the far field is enhanced along the axial direction with an inverse  $\sqrt{r}$  dependence. In this AEFf situation, the far field on the axis [i.e.,  $\mathbf{r} = (0, 0, z)$  with a positive  $z$ , say] will be considered first; from the previous considerations, there are two cases to study, and in Secs. III A and III B each will be treated separately. Section III C is devoted to the calculation of the far field in the neighborhood of the axis.

### A. AEFF on axis from a ring of stationary phase

Here the points of stationary phase are determined by the extremum point on the  $n_z$ - $n_x$  curve (or the  $n_z$ - $n_1$  curve for any one  $\phi$ ) at a nonzero  $n_x$  (or  $n_1$ ) as given by Eq. (5); they obviously form a ring about the  $z$  axis. Because  $\lambda_\phi=0$  and subsequently  $K=0$ , Eq. (15) no longer applies. One has to go back to Eq. (6). In terms of the parametric coordinates  $(n_1, \phi)$ , the phase factor within the surface integral can be Taylor-series-expanded about any point  $(v_1, \phi)$  on the ring as

$$k_z z = [v_z + v_z''(n_1 - v_1)^2/2]z\omega/c, \quad (17)$$

which is independent of  $\phi$ , where  $v_z'' = d^2 n_z / dn_1^2$  at  $v_1$ . The integration over  $n_1$  for large  $z$  can now be performed by means of the method of stationary phase and we obtain an inverse- $z^{1/2}$ -dependent field:

$$E(z) = \{G \exp[i(\kappa_z z \pm \pi/4)] / (\omega z/c)^{1/2}\} \langle \vec{\Gamma} \cdot \mathbf{J} \rangle, \quad (18)$$

where  $\kappa_z = \omega v_z/c$ ,

$$\langle Q \rangle = (1/2\pi) \int_0^{2\pi} d\phi Q$$

is the average of  $Q$  over the azimuthal angle  $\phi$ ,

$$G = (8\pi)^{1/2} \omega^2 v_1 / (c^3 |v_z''|^{1/2} \partial \mathcal{D} / \partial n_z) \quad (19)$$

is a coefficient evaluated at  $v_1$ , and the positive (negative)  $\pi/4$  phase is taken if the WS is topologically a two-sheeted hyperboloid (an ellipsoid). For reference, we write down the values of  $v_z''$  and  $\partial \mathcal{D} / \partial n_z$ :

$$v_z'' = [-(1+S/P) \pm (h''/2 - h'^2/4h) / \sqrt{h}] / 2v_z, \quad (20)$$

which equals  $\lambda_1$  at  $v_1$ , and

$$\frac{\partial \mathcal{D}}{\partial n_z} = \pm 4v_z \sqrt{h} P, \quad (21)$$

where  $h$  is given by Eq. (1b),  $h'$  and  $h''$  are derivatives with respect to  $n_x$ , all evaluated at  $n_x = v_1$  and  $n_z = v_z$  given by Eqs. (5a) and (5b). Again, there appear two values of  $v_z''$  in Eq. (20). To determine which is the proper one, we again note that, in Fig. 2, as the boundary line  $R = -P$  or  $L = -P$  is approached by any parameter point in a nearby subdomain of AEFF, the proper  $v_z''$  will tend to zero. This criterion leads to the choice of the plus sign in Eq. (20) for subdomains 4a, 7c, 8b, 11a, and 13c, whereas it leads to the choice of the minus sign for 7a and 13a.

To evaluate the  $\phi$  integral, we assume an electric dipole source of dipole moment  $\mathbf{p}$  so that

$$\mathbf{J}(\mathbf{k}) = -i\omega \mathbf{p}. \quad (22)$$

Being independent of  $\mathbf{k}$ ,  $\mathbf{J}$  can be taken out of the average operation. Obviously, Eq. (8) leads to

$$\begin{aligned} \langle \Gamma_{xx} \rangle &= \langle \Gamma_{yy} \rangle = a_1 + a_2/2, \\ \langle \Gamma_{xy} \rangle &= \langle \Gamma_{yx}^* \rangle = ia_3, \\ \langle \Gamma_{zz} \rangle &= a_6, \end{aligned} \quad (23)$$

other elements being zero. If the source is a linear dipole,

we may take  $\mathbf{p} = (p_x, 0, p_z)$  and the far field at  $(0, 0, z)$  is therefore given by Eq. (18) with the components of  $\langle \vec{\Gamma} \cdot \mathbf{J} \rangle$  being

$$\begin{aligned} \langle \vec{\Gamma} \cdot \mathbf{J} \rangle_x &= -i\omega p_x (a_1 + a_2/2), \\ \langle \vec{\Gamma} \cdot \mathbf{J} \rangle_y &= -\omega p_x a_3, \\ \langle \vec{\Gamma} \cdot \mathbf{J} \rangle_z &= -i\omega p_z a_6, \end{aligned} \quad (24)$$

with the  $a$ 's given by Eq. (9) evaluated at  $v_1$ . We see that the enhanced (total) far field on the  $z$  axis is transverse or longitudinal according to the dipole source being perpendicular or parallel to the external magnetic field, respectively. In the latter case, the parallel oscillation is at frequencies *below* the plasma frequency. However, this parallel electric field oscillation, being valid only on the axis, by no means contradicts the well-known result that there is no *plane*-wave oscillation parallel to the field in a cold magnetoplasma below the plasma frequency. The cause of this longitudinal oscillation may be described as follows. The dipole source is parallel to  $\mathbf{B}_0$ ; all the excited waves with their wave vectors ending on the ring of stationary phase are thus of *equal* magnitude and phase when reaching the observer at  $z$ . Each wave field has a component parallel as well as a component perpendicular to  $\mathbf{B}_0$ . From cylindrical symmetry, all the perpendicular components cancel one another while the parallel components add up to give the resultant longitudinal electric field.

We now come to explain the origin of the  $1/\sqrt{z}$  dependence. This is not difficult to do in view of the explanation of the  $1/r$  dependence following Eq. (16). The phase given by Eq. (17) is independent of the azimuthal angle  $\phi$ ; this immediately indicates that, while the effective length along the  $n_1$ -coordinate line is  $(\lambda_1 z)^{-1/2}$  or  $(v_z'' z)^{-1/2}$  as in the normal case, the effective length along the  $\phi$ -coordinate line is the whole length of the ring and there is no restriction from the distance  $z$ . Physically, this means that all the plane sinusoidal waves with wave vectors ending on the ring contribute to the far field on an *equal footing* and they reach the observer at  $z$  with the *same phase*. The effective area is therefore equal to the product of  $(v_z'' z)^{-1/2}$  and  $2\pi v_1$ , leading to the inverse  $\sqrt{z}$ -dependent result as given by Eq. (18).

Finally, we would like to discuss the state of polarization of the wave field in the  $xy$  plane. From Eq. (24),

$$E_y / iE_x = -a_3 / (a_1 + a_2/2), \quad (25)$$

which must tend to 1 (or  $-1$ ) as the  $R = -P$  (or  $L = -P$ ) boundary line in Fig. 2 is approached by any parameter point. Numerically, we have found that  $E_y / iE_x$  keeps its sign within any subdomain of AEFF and we may conclude that the  $R$ -type (or  $L$ -type) AEFF is right-handed (or left-handed) as far as the state of polarization in the  $xy$  plane is concerned.

### B. AEFF on axis from the quasiflat pole

We now turn to the case where the derivatives of  $k_z$  with respect to  $k_x$  at the origin are zero up to the third order. This happens when the plasma parameter point

sits exactly on one of the  $R = -P$  and  $L = -P$  lines in Fig. 2. The Gaussian curvature at the pole of the WS is obviously zero. Again we have to go back to Eq. (6). Using  $n_x$  and  $n_y$  as the parametric coordinates for the surface, expanding  $k_z$  in the phase factor according to Eq. (4a) with  $n_x^2$  replaced by  $n_z^2$ , the integration can again be done according to the standard method of stationary phase and the result, also inversely  $z^{1/2}$  dependent, is

$$\mathbf{E}(z) = \mathbf{E}_p \exp[i(\omega|P|^{1/2}z/c \pm \pi/4)] / (\omega z/c)^{1/2}, \quad (26)$$

with

$$\mathbf{E}_p = \frac{\omega^2}{c^3} \left[ \frac{\pi}{|\alpha|} \right]^{1/2} \vec{\Gamma} \cdot \mathbf{J} / \frac{\partial \mathcal{D}}{\partial n_z}, \quad (27)$$

where the whole expression is evaluated at  $n_\perp = 0$ ,  $\alpha$  is given by Eq. (4b), the upper positive (lower negative) sign in the phase is taken if the WS is a two-sheeted hyperboloid (an ellipsoid), and the relation  $n_z = \sqrt{|P|}$  has been used. The actual evaluation of  $\vec{\Gamma} \cdot \mathbf{J}$  and  $\partial \mathcal{D} / \partial n_z$  at  $n_\perp = 0$  and  $k_z = \omega \sqrt{|P|} / c$  are quite simple and Eq. (27) thus reduces to

$$\mathbf{E}_p = -\frac{\sqrt{\pi}}{4} \frac{\omega^2}{c^3} \left[ \frac{D^2 |P|}{S^2} \right]^{1/4} J_x(\hat{\mathbf{x}} \pm i\hat{\mathbf{y}}), \quad (28)$$

where the current density has been assumed lying in the  $xz$  plane, and the plus (or minus) sign is for the  $R = -P$  (or  $L = -P$ ) case. Since the far field comes from the surface element at the pole of the WS or from the plane waves propagating along the external magnetic field, it is circularly polarized as expected.

The origin of the inverse  $\sqrt{z}$  dependence again lies in the method of the stationary phase. Because the surface around the pole is flatter, there are more plane sinusoidal waves arriving at  $z$  with the same phase. The effective area is  $(|\alpha|z)^{-1/2}$  [each effective length being about  $1/(|\alpha|z)^{1/4}$ ], larger than for an ordinary pole with a nonzero Gaussian curvature. This explains the proper dependence of the far field on the distance.

Note that Eq. (18) does not lead to Eq. (26) if the  $\nu_1 \rightarrow 0$  limit is taken. This could be explained by the fact that only terms up to the second order had been kept in the derivation [see Eq. (17)]; as  $\nu_1$  tends to zero and the parameter point in the CMA diagram approaches the  $R = -P$  (or  $L = -P$ ) boundary line,  $\nu_z''$  at the point of the stationary phase itself becomes vanishingly small and the higher-order terms can no longer be neglected. In other words, the result of Eq. (18) is valid only *within* the subdomains of AEF. In Appendix A, consideration beyond the method of stationary phase is made and the connection between the results in the two cases is shown.

### C. AEF around the axis from a ring of stationary phase

We now consider the far field *around* the  $z$  axis. If the observation point  $\mathbf{r}$  is written as  $(r_\perp \cos\Phi, r_\perp \sin\Phi, z)$  in cylindrical coordinates, the phase in Eq. (6) becomes

$$\mathbf{k} \cdot \mathbf{r} = k_z z + k_\perp r_\perp \cos(\phi - \Phi). \quad (29)$$

Given a finite  $r_\perp$  and for a sufficiently large  $z$ , one can

again apply the method of stationary phase to the  $k_\perp$ —or  $n_\perp$ —integral (see Appendix B for more details). For the case of a ring of stationary phase at  $\nu_\perp \neq 0$  on the WS and for a dipole source, the electric far field is

$$\mathbf{E}(\mathbf{r}) = \frac{G \exp[i(\kappa_z z \pm \pi/4)]}{(\omega z/c)^{1/2}} \vec{\Pi} \cdot \mathbf{J}, \quad (30)$$

where  $G$  is given by Eq. (19) and with  $\kappa_\perp = \nu_\perp \omega/c$

$$\vec{\Pi} = \langle \vec{\Gamma} \exp[i\kappa_\perp r_\perp \cos(\phi - \Phi)] \rangle \quad (31)$$

and  $\mathbf{J}$  has been taken out of the average operation because of its  $\mathbf{k}$  independence. Subsequent evaluations are readily carried out in terms of the Bessel functions  $J_n(\xi)$ 's and the results are

$$\begin{aligned} \Pi_{xx} &= (a_1 + a_2/2)J_0(\xi) \\ &\quad - a_2[J_0(\xi)/2 + J_0''(\xi)]\cos(2\Phi), \end{aligned} \quad (32a)$$

$$\begin{aligned} \Pi_{yy} &= (a_1 + a_2/2)J_0(\xi) \\ &\quad + a_2[J_0(\xi)/2 + J_0''(\xi)]\cos(2\Phi), \end{aligned} \quad (32b)$$

$$\begin{aligned} \Pi_{xy} &= \Pi_{yx}^* \\ &= ia_3 J_0(\xi) - a_2[J_0(\xi)/2 + J_0''(\xi)]\sin(2\Phi), \end{aligned} \quad (32c)$$

$$\Pi_{xz} = -\Pi_{zx}^* = [a_4 \sin\Phi + ia_5 \cos\Phi]J_1(\xi), \quad (32d)$$

$$\Pi_{yz} = -\Pi_{zy}^* = [-a_4 \cos\Phi + ia_5 \sin\Phi]J_1(\xi), \quad (32e)$$

$$\Pi_{zz} = a_6 J_0(\xi), \quad (32f)$$

where  $\xi \equiv \kappa_\perp r_\perp$  and  $J_0''(\xi) = d^2 J_0(\xi) / d\xi^2$ . Note that

$$J_0(\xi) \rightarrow 1,$$

$$J_1(\xi) \rightarrow 0,$$

$$J_0''(\xi) \rightarrow -1/2,$$

as  $r_\perp$  or  $\xi$  tends to zero, the elements in Eq. (32) reduce to those in Eq. (23) as expected. We therefore see that the strength of the enhanced far field, of  $1/\sqrt{z}$  dependence along the axis, varies essentially as  $J_0(\kappa_\perp r_\perp)$  in the transverse direction, meaning that the AEF is confined to an area of radius of the order of the transverse wavelength  $\kappa_\perp^{-1}$ .

## IV. RADIATION ENERGY FLUX

Since a cold magnetoplasma is spatially nondispersive, the energy flux density is simply given by the Poynting vector. For the case of AEF from the quasiflat pole as discussed in Sec. III B, the corresponding wave magnetic field is merely  $n_z \hat{\mathbf{z}} \times \mathbf{E}$ , and thus the time-averaged Poynting vector, being the real part of  $c(\mathbf{E} \times \mathbf{B}^*) / 8\pi$ , is easily obtained to be

$$\mathbf{S}(z) = c^2 |P|^{1/2} |\mathbf{E}_p|^2 \hat{\mathbf{z}} / (8\pi\omega z) \quad (33)$$

on the  $z$  axis where  $\mathbf{E}_p$  is given by Eq. (28) and  $n_z = |P|^{1/2}$  has been substituted.

As for the case of AEF from a ring of stationary phase, the wave magnetic field cannot be obtained as sim-

ply because waves of different wave vectors are involved. However, it can still be obtained in a straightforward way from Faraday's law  $\mathbf{B} = c \nabla \times \mathbf{E} / i\omega$ , with  $\mathbf{E}$  given by Eq. (6) or Eqs. (30) and (31). To  $1/\sqrt{z}$  order, the magnetic field can be written as

$$\mathbf{B}(\mathbf{r}) = v_z \hat{\mathbf{z}} \times \mathbf{E}(\mathbf{r}) + \frac{G v_1 \exp[i(\kappa_2 z \pm \pi/4)]}{(\omega z / c)^{1/2}} \vec{\Sigma} \cdot \mathbf{J}, \quad (34)$$

where  $\vec{\Sigma} \equiv \langle \hat{\rho} \times \vec{\Gamma} \exp[i\kappa_1 r_1 \cos(\phi - \Phi)] \rangle$ , an average over the azimuthal angle  $\phi$  in the wave-vector space, has the following components:

$$\Sigma_{xx} = ia_4 J_0(\xi)/2 + [ia_4 \cos(2\Phi) - a_5 \sin(2\Phi)] \times [J_0(\xi)/2 + J_0''(\xi)], \quad (35a)$$

$$\Sigma_{yy} = ia_4 J_0(\xi)/2 - [ia_4 \cos(2\Phi) - a_5 \sin(2\Phi)] \times [J_0(\xi)/2 + J_0''(\xi)], \quad (35b)$$

$$\Sigma_{zz} = \Sigma_{xx} + \Sigma_{yy}, \quad (35c)$$

$$\Sigma_{xy} = a_5 J_0(\xi)/2 + [ia_4 \sin(2\Phi) + a_5 \cos(2\Phi)] \times [J_0(\xi)/2 + J_0''(\xi)], \quad (35d)$$

$$\Sigma_{yx} = -a_5 J_0(\xi)/2 + [ia_4 \sin(2\Phi) + a_5 \cos(2\Phi)] \times [J_0(\xi)/2 + J_0''(\xi)], \quad (35e)$$

$$\Sigma_{xz} = ia_6 \sin\Phi J_1(\xi), \quad (35f)$$

$$\Sigma_{zx} = [-ia_1 \sin\Phi + a_3 \cos\Phi] J_1(\xi), \quad (35g)$$

$$\Sigma_{yz} = -ia_6 \cos\Phi J_1(\xi), \quad (35h)$$

$$\Sigma_{zy} = [ia_1 \cos\Phi + a_3 \sin\Phi] J_1(\xi). \quad (35i)$$

Since both  $\mathbf{E}$  and  $\mathbf{B}$  fields depend on the Bessel functions, we see immediately that the radiation flux, if it exists, will be confined to the axis with a cross-sectional area roughly equal to the square of the transverse wavelength  $\kappa_1^{-1}$ . The actual evaluation of the time-averaged Poynting vector, on the other hand, is quite a tedious matter. However, if we limit ourselves to the immediate region around the axis so that only terms up to the first order in  $\xi = \kappa_1 r_1$  in the expansion of the Bessel functions need to be kept, the expressions for  $\mathbf{E}$  and  $\mathbf{B}$  can be substantially simplified. In what follows, we shall write down such simplified results for three orientations of the dipole source.

(i) For a dipole source parallel to  $\mathbf{B}_0$ , i.e.,  $\mathbf{p} = p \hat{\mathbf{z}}$ , the time-averaged Poynting vector is

$$\mathbf{S} = \frac{(cGp\omega)^2}{16\pi\omega z} \kappa_1 a_4 (v_1 a_5 - a_6 v_2) (y \hat{\mathbf{x}} - x \hat{\mathbf{y}}). \quad (36)$$

Note that  $\mathbf{S}$  is zero on the axis; this is expected in view of the existence of only a parallel electric far field on the axis. However, the fact that  $\mathbf{S} = 0$  while  $\mathbf{E} \neq 0$  on the axis raises an interesting question on the relation between wave energy flux density  $\mathbf{S}$  and wave energy density  $U$ . All the waves contributing to the far field do have the same and nonzero group velocity parallel to the  $z$  axis, but since their wave vectors, which end on the ring of a finite radius, could differ by a finite amount, the usual relation  $\mathbf{S} = \mathbf{V}_g U$  no longer holds. Note also that the transverse divergence  $\nabla_{\perp} \cdot \mathbf{S}_{\perp}$  is zero and, in fact, the energy flux lines form circles, indicating circular energy flow around the axis.

(ii) For a dipole perpendicular to  $\mathbf{B}_0$  and lying along the  $x$  axis, i.e.,  $\mathbf{p} = p \hat{\mathbf{x}}$ , we have

$$\mathbf{S} = \frac{(cGp\omega)^2}{16\pi\omega z} \left\{ \left[ v_1 \left[ a_1 a_3 - \frac{a_4 a_5}{2} \right] + v_z a_4 \left[ a_1 + \frac{a_2}{2} \right] \right] \kappa_1 y \hat{\mathbf{x}} - \left[ v_1 \left[ a_1 a_3 - \frac{a_4 a_5}{2} + \frac{a_2 a_3}{2} \right] - v_z a_3 a_5 \right] \kappa_1 x \hat{\mathbf{y}} + \left[ v_1 \left[ a_3 a_4 - a_1 a_5 - \frac{a_2 a_5}{2} \right] + 2v_z \left[ a_1 + \frac{a_2}{2} \right]^2 + 2v_z a_3^2 \right] \hat{\mathbf{z}} \right\}. \quad (37)$$

This time  $S_z$ , being  $1/z$  dependent, is much stronger than a usual  $1/r^2$ -dependent radiation flux. On the other hand,  $\nabla_{\perp} \cdot \mathbf{S}_{\perp} = 0$  is still true, though the energy does not necessarily flow in circles about the axis.

(iii) For a dipole circling the  $xy$  plane, i.e.,  $\mathbf{J} = -i\omega p(\hat{\mathbf{x}} \pm i \hat{\mathbf{y}})$ , we have

$$\mathbf{S} = \frac{(cGp\omega)^2}{8\pi\omega z} \left\{ \frac{\kappa_1}{2} \left[ v_z (a_4 \pm a_5) \left[ a_1 + \frac{a_2}{2} \mp a_3 \right] \mp \frac{v_1}{2} (a_4 \pm a_5)^2 + v_1 \left[ a_1 + \frac{a_2}{2} \mp a_3 \right] (a_3 \mp a_1) \right] (y \hat{\mathbf{x}} - x \hat{\mathbf{y}}) + 2 \left[ v_z \left[ a_1 + \frac{a_2}{2} \mp a_3 \right]^2 \mp \frac{v_1}{2} (a_4 \pm a_5) \left[ a_1 + \frac{a_2}{2} \mp a_3 \right] \right] \hat{\mathbf{z}} \right\}. \quad (38)$$

Again we have a much enhanced energy flow along the axial direction, but the transverse flux lines, different from those in case (ii), are now circular about the axis as perhaps expected from cylindrical symmetry consideration. The actual radiation flux therefore flows helically forward and degenerates to a pure axial flow on the axis.

We are now in a position to discuss the  $1/z$  dependence

of the radiation flux in relation to the law of energy conservation. Since we have been considering a steady-state source, we must require

$$\nabla \cdot \mathbf{S}_T = 0, \quad (39)$$

where  $\mathbf{S}_T$  refers to the total energy flux density. What we have just obtained is of the following form:

$$\mathbf{S} = (\mathbf{F}_\perp + F_z \hat{\mathbf{z}}) / z, \quad (40)$$

where  $\mathbf{F}_\perp$  and  $F_z$  are  $z$  independent; it is not divergence-free. This is because only dominant terms, of the order of  $1/z$ , have been kept. Including the subdominant terms of relevance, we may write

$$\mathbf{S} = (\mathbf{F}_\perp + F_z \hat{\mathbf{z}}) / z + (\mathbf{f}_\perp + f_z \hat{\mathbf{z}}) / z^2, \quad (41)$$

with  $\mathbf{f}_\perp$  and  $f_z$  again  $z$  independent. The requirement of a divergence-free Poynting vector at each level of  $1/z$  implies

$$\nabla \cdot \mathbf{F}_\perp = 0, \quad (42)$$

$$F_z = \nabla \cdot \mathbf{f}_\perp. \quad (43)$$

While we have seen the validity of Eq. (42) in our results so far obtained, Eq. (43) can be used to obtain  $\mathbf{f}_\perp$  as follows. Noticing that  $F_z$  is constant in the immediate region around the axis, we have, good to first order in  $r_\perp$ ,

$$f_x = C_x x, \quad (44a)$$

$$f_y = C_y y, \quad (44b)$$

where  $C_x + C_y = F_z$ . Disregarding, for the moment, the contribution from  $\mathbf{F}_\perp$  which itself conserves energy, the energy flux lines in the  $xz$  plane and the  $yz$  plane are described by

$$z = \text{const} \times x^{F_z/C_x}, \quad (45a)$$

$$z = \text{const} \times y^{F_z/C_y}, \quad (45b)$$

respectively. In particular, for the cylindrically symmetric case,  $C_x = C_y = F_z/2$ , the flux line varies as

$$z = \text{const} \times r_\perp^2. \quad (46)$$

The actual flux lines, besides circling about the axis according to the  $\mathbf{F}_\perp$  term, are therefore curved from the radial direction towards the axis, but they are nevertheless pointing outward, both transversely and axially. Note that, in the absence of cylindrical symmetry, we may introduce an averaged transverse outflow as

$$\langle f_r \rangle = \int_A \mathbf{f}_\perp \cdot d\mathbf{a} / A = \int_0^{2\pi} d\phi f_r / 2\pi, \quad (47)$$

where  $A$  is a small cylindrical surface area about the axis. It is then not difficult to show that

$$\langle f_r \rangle = r_\perp F_z / 2. \quad (48)$$

The energy flux line, in the averaged sense, is again given by Eq. (46).

## V. CONCLUSIONS AND FURTHER REMARKS

In this paper we have classified the plasma parameter domains in the CMA diagram where an axially enhanced far field exists. Such an AEF depends on distance in an inverse square-root manner and is found confined within a constant cross section in most cases. Its origin has been explained and its associated radiation characteristics have been obtained and discussed. The existence of an AEF parallel to the axis and oscillating below the plas-

ma frequency has also been noted.

From the CMA classification, the axial enhancement of the far field is a common occurrence (especially in the low-frequency regime) and should be of experimental relevance. Furthermore, knowledge about it may be useful in the understanding of field-aligned radiation phenomena (such as whistler ducting, pulsar radiation, etc.) from a new perspective.

## APPENDIX A

To get an idea of the relation between the two results in Eqs. (18) and (26), the radius of the ring of extrema on the WS is assumed so small that the integrand in Eq. (6), except the exponential function, may be approximated by the value at the pole, and the resultant surface integral essentially takes the following form:

$$I = 2\pi \int_0^N k_\perp dk_\perp \exp(ik_z z),$$

where  $k_z = k_{z0} + bk_\perp^2 + ak_\perp^4$  is valid, with real constants  $a, b$  satisfying  $b/a < 0$ , and furthermore,  $N > (-b/2a)^{1/2}$ , meaning that the integration domain includes the position of the extremum.

By changing the integration variable to  $\eta \equiv k_\perp^2 + b/2a$ , we may rewrite  $I$  as

$$I = \pi \exp[i(k_{z0} - b^2/4a)z] \times \left[ \int_0^{N^2 + b/2a} d\eta e^{iaz\eta^2} + \int_0^{|b/2a|} d\eta e^{iaz\eta^2} \right].$$

If  $b=0$  exactly, only the first integral survives and, for  $(z|a|)^{1/2} \gg 1/N^2$ , it gives rise to the result as obtained in Eq. (26). If  $b \neq 0$ , both integrals have to be considered; for  $(z|a|)^{1/2} \gg 1/(N^2 - |b/2a|)$  and  $(z|a|)^{1/2} \gg |2a/b|$ , each integral contributes an equal amount and the total gives rise to the ring result in Eq. (18). For a very small  $b$ , the second inequality as required above may not hold and Eq. (18) is no longer good. However, the second integral can be expressed in terms of the Fresnel integral

$$\mathcal{F}_\pm(x) \equiv \frac{2}{\sqrt{\pi}} \int_0^x e^{\pm it^2} dt,$$

and we have

$$I = \frac{\pi^{3/2}}{2(|a|z)^{1/2}} e^{ik_{z0}z} \{ \exp[i \text{sgn}(a)\pi/4] + \mathcal{F}_{\text{sgn}(a)}((b^2z/4|a|)^{1/2}) \},$$

where  $\text{sgn}(a) \equiv a/|a|$ . Knowing the series expansion and the asymptotic expression of the Fresnel integral, this formula obviously connects the results in Eqs. (18) and (26).

## APPENDIX B

To evaluate the far-field integral in Eq. (6) with the given phase in Eq. (29), the contribution from an integral domain of width  $2\Delta$  around a point  $\kappa_\perp$  is considered:

$$\Delta I = \int_0^{2\pi} d\phi \int_{\kappa_1 - \Delta}^{\kappa_1 + \Delta} dk_{\perp} \exp \left[ i \left[ \kappa_z + \kappa'_z (k_{\perp} - \kappa_1) + \frac{\kappa''_z}{2} (k_{\perp} - \kappa_1)^2 \right] z + ik_{\perp} r_1 \cos(\phi - \Phi) \right] Q(k_{\perp}, \phi),$$

where  $|\kappa''_z| \Delta \ll |\kappa'_z|$  has been assumed in the expansion. For sufficiently large  $z$  while  $r_1$  remaining finite, the contribution from the domain where  $\kappa'_z = 0$  is again dominant. In particular, if  $|\kappa''_z z|$  is assumed much greater than  $\Delta^{-2}$  and  $r_1^2$ , the dominant contribution can be obtained in a straightforward way and the result is that given in Sec. III C. The condition for applicability is therefore that the axial distance  $z$  has to be much larger than the absolute values of  $(\kappa''_z)^2 / (\kappa'_z)^3$  and  $r_1^2 / \kappa'_z$ .

---

<sup>1</sup>M. J. Lighthill, *Philos. Trans. R. Soc. London, Ser. A* **252**, 397 (1960).

<sup>2</sup>M. J. Giles, *J. Plasma Phys.* **19**, 201 (1978).

<sup>3</sup>H. H. Kuehl, *Phys. Fluids* **5**, 1095 (1962).

<sup>4</sup>N. Singh and R. W. Gould, *Phys. Fluids* **16**, 75 (1973).

<sup>5</sup>T. H. Stix, *The Theory of Plasma Waves* (McGraw-Hill, New York, 1962), Chaps. I and II.

<sup>6</sup>H. M. Lai and P. K. Chan, *Phys. Fluids* **29**, 1881 (1986).